Journal of Power Sources 243 (2013) 147–151

Contents lists available at SciVerse ScienceDirect

Journal of Power Sources

journal homepage: www.elsevier.com/locate/jpowsour

Short communication

Synthesis and electrochemical properties of $LiFeP_{1-x}B_xO_{4-\delta}$/C cathode materials

Zhang Lu [a,b,c], Kang Xueya [a,c,*], Tuerdi Wumair [a,c], Dou Junqing [a,b,c], Han Ying [a,c]

[a] Xinjiang Technical Institute of Physics and Chemistry, Chinese Academy of Sciences, Urumqi 830011, China
[b] Graduate University of Chinese Academy of Sciences, Beijing 100049, China
[c] Xinjiang Key Laboratory of Electronic Information Materials and Devices, Urumqi 830011, China

HIGHLIGHTS

- The composite materials of B-doped $LiFeP_{1-x}B_xO_{4-\delta}$/C ($x$ = 0.00, 0.05, 0.10 and 0.15) are synthesized.
- It is possible to reduce sintering time and sintering temperature in liquid phase reduction method.
- The samples all have well-regulated olivine-type structures, high crystalinity.
- The B-doping materials have improved the conductivity of composite materials, decreased the polarization of electrode.
- The B-doping materials enhance the cycling performance and high rate capability effectively.

ARTICLE INFO

Article history:
Received 25 December 2012
Received in revised form
20 May 2013
Accepted 20 May 2013
Available online 31 May 2013

Keywords:
Lithium-ion battery
Cathode material
Lithium iron phosphate
B-Doping

ABSTRACT

The composite materials of B-doped $LiFeP_{1-x}B_xO_{4-\delta}$/C ($x$ = 0.00, 0.05, 0.10 and 0.15) at P-site are synthesized in flowing N_2 atmosphere by liquid phase reduction method with heat treatment. The synthesized products are characterized by X-ray diffraction, SEM, cyclic voltammetry and galvanostatic charge/discharge tests. The results show that the samples all have well-regulated olivine-type structures, high crystallinity, moderate and uniform particle size, while B-doping improves the conductivity of composite materials, decreases the polarization of electrode, and enhances the cycling performance and high rate capability effectively. The $LiFeP_{0.9}B_{0.1}O_{4-\delta}$/C composite exhibits the best electrochemical performance in the all samples. The discharge capacities of $LiFeP_{0.9}B_{0.1}O_{4-\delta}$/C are 155.2 mAh g^{-1}, 146.2 mAh g^{-1}, 139.4 mAh g^{-1}, 132.4 mAh g^{-1}, 119.1 mAh g^{-1} and 102.6 mAh g^{-1} at the rate of 0.2C, 0.5C, 1.0C, 2.0C, 5.0C, and 10.0C.

1. Introduction

Lithium ion batteries potentially provide a solution for the future energy economy as the low-cost, environmental friendly, less toxic, long cycle-life and excellent electrochemical performance, etc. [1]. And the batteries have been utilized for energy storage in mobile, laptop and electric bicycle, etc. [2].

Since the pioneering work of Padhi and co-workers in 1997 [3], $LiFePO_4$ has been considered as a successful polyanionic intercalation cathode material due to the advantages of high theory capacity (~170 mAh g^{-1}), excellent thermal stability, no toxicity and low cost, high reversibility, etc. The strong covalent bonds between oxygen and phosphorus ions in PO_4^{3-} tetrahedral polyanions give the high stability and the high reversibility of the $LiFePO_4$. However, the diffusion of the Li^+ ions is inhibited due to the strong P–O bonds (the intrinsic Li^+ ions conductivity of $LiFePO_4$ is lower than 2×10^{-14} cm^2 S^{-1} [4]). Therefore, the problem of the low Li^+ ions conductivity is considered the main barrier used in large-scale manufacture of $LiFePO_4$ [5].

At present, many methods have been used to increase the conductivity of the Li^+ ions such as doping and minimizing particle size. The doping is considered the most effective method to increase the Li^+ ions conductivity. The ion doping modification research mainly focused on Li site and Fe site, such as Na^+, Mn^{2+}, Ti^{4+} and V^{5+} [6–11]. But there are few reports about ion doping at P site or O site. Zhang Yurong et al. [12] reported that Ti, Cu and Nb was doped into the Fe site and the P site, respectively, to synthesize olivine structure $Li_{2+2x}Ti_{1-x}Cu_x(NbO_4)_2$. Its conductivity is 1.26×10^{-5} S cm^{-1}, much

* Corresponding author. Xinjiang Technical Institute of Physics and Chemistry, Chinese Academy of Sciences, Urumqi 830011, China. Tel.: +86 0991 3850517; fax: +86 0991 3838957.
E-mail addresses: xueyakang@yahoo.cn, xueyakang@126.com (K. Xueya).

0378-7753/$ – see front matter © 2013 Elsevier B.V. All rights reserved.
http://dx.doi.org/10.1016/j.jpowsour.2013.05.093

higher than $LiFePO_4$. The result indicated that P-site doping also is an effective way for increase the Li^+ ions conductivity, and then improving the electrochemical performances of $LiFePO_4$.

$LiFeBO_3$ as a new cathode material, it has a higher theoretical capacity (220 mAh g^{-1}) and higher Li^+ ions conductivity (3.9×10^{-7} S cm^{-1}) than $LiFePO_4$. These are all due to the light molecular weight of $(BO_3)^{3-}$ and special structure of the $LiFeBO_3$ [13–16]. In the crystal structure of the $LiFeBO_3$, the LiO_5, FeO_5 and BO_3 will not form edge-sharing structure as $LiFePO_4$. At the same time, the bond of B–O is weaker than P–O bond. So the Li^+ ions could be moved more smoothly in $LiFeBO_3$ crystal than in $LiFePO_4$. Therefore, we attempted to increase the Li^+ ions conductivity than improving the electrochemical performances of $LiFePO_4$ by doping B ions at P site.

In this paper, $LiFeP_{1-x}B_xO_{4-\delta}/C$ ($x = 0.00$, 0.05, 0.10 and 0.15) are synthesized in flowing N_2 atmosphere by liquid phase reduction method with heat treatment. The effect of the B ions doping at P site on $LiFePO_4$ electrochemical performances is discussed in detail.

2. Materials and methods

2.1. Synthesis of the materials

$LiFeP_{1-x}B_xO_{4-\delta}/C$ ($x = 0.00$, 0.05, 0.10 and 0.15) were synthesized in flowing N_2 atmosphere by liquid phase reduction method with heat treatment in experiment. All the reagents used in experiment were of analytical purity and used without further purification. $LiOH \cdot H_2O$, $FePO_4 \cdot 2H_2O$, H_3BO_3 were used as starting materials, $C_6H_{10}O_4$ and oxalic acid as carbon source material (with the total amounts of 10 wt% for the final products) and deoxidizer, respectively. Stoichiometric amounts of the starting materials were dissolved in deionized water, under strongly stirred and water bath heating (the temperature was 80 °C) for 4 h. After drying at 80 °C in oven, the mixture was ground and pressed into a pillet. Then the pillet was sintered at 700 °C for 2 h in a tube furnace under nitrogen atmosphere. After cooling to room temperature, the final product—$LiFeP_{1-x}B_xO_{4-\delta}/C$ ($x = 0.00$, 0.05, 0.10 and 0.15) were obtained.

2.2. Characterization of the materials

The XRD patterns were collected using a Rigaku RINT-2500V X-ray diffractometer equipped with Cu $K\alpha$ radiation ($\lambda = 1.5418$ Å) by step scanning in the 2θ range of 10°–70°.

The scanning electron microscopy (SEM) images of the composite were collected under an accelerating voltage of 5 kV on a Zeiss Supra55(VP) scanning electron microscope.

2.3. Cell assembly and electrochemical tests

Electrochemical cells were configured in the following way: the synthesized powder was mixed with 10% acetylene black and 10% polyvinylidene fluoride (PVDF) in 1-methyl-1-pyrrolidinone to form slurry. Subsequently, the mixed slurry was pasted onto an aluminum foil, and dried at 120 °C for 12 h in a vacuum box. The electrolyte was 1 M $LiPF_6$ in a mixture of ethylene carbonate (EC), ethyl methyl carbonate (EMC) and dimethyl carbonate (DMC) with a volume ratio of 1:1:1. A test cell consisted of the cathode and lithium foil anode separated by a porous polypropylene film (Celgard 2400). The assembly of the test cells (CR2025) was carried out in a dry Ar-filled glove box.

The charge–discharge measurements were performed at room temperature in the voltage range of 2.3–4.3 V using a computer controlled multi-channel battery test system (BTS-51, Neware, China). Cyclic voltammogram (CV) test was performed on electrochemical workstation (CHI650C, Shanghai, China) over a voltage range of 2.3–4.3 V at the scan rate of 0.1 mV s^{-1}.

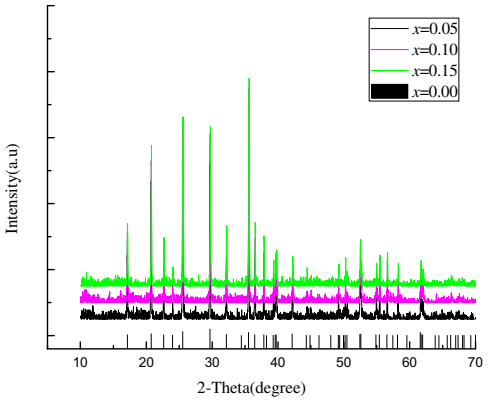

Fig. 1. X-ray diffraction patterns of $LiFeP_{1-x}B_xO_{4-\delta}/C$ ($x = 0.00$, 0.05, 0.10 and 0.15) samples.

3. Results and discussion

3.1. Material characterizations

Fig. 1 shows the XRD patterns of the obtained $LiFeP_{1-x}B_xO_{4-\delta}/C$ ($x = 0.00$, 0.05, 0.10 and 0.15) samples. The strong and narrow diffraction peaks indicate that the well crystallized orthorhombic olivine-type structure was successfully obtained in experiment. At the same time, there are no other impurity phases such as carbon peaks can be found in either of these XRD patterns. That's because the low carbon content and the amorphous state of the carbon in these samples. Therefore the doping ions of B at P-site didn't destroy the crystal structure of the $LiFePO_4$.

As for the B-doped $LiFePO_4/C$, there exists another impurity phase of $LiFeBO_3/C$ at the positions of $2\theta = 24.3°$and 44.7° [16]. As we can see that the composite materials of B-doped $LiFePO_4/C$ at P-site are synthesized, and the solid solution of $LiFeP_{1-x}B_xO_{4-\delta}$ consists of $LiFePO_4$ and $LiFeBO_3$. Therefore the doping ions of B at P-site didn't destroy the crystallized orthorhombic olivine-type structure of the $LiFePO_4$.

The calculated lattice constants of B-doped $LiFePO_4/C$ obtained from the refinement result are summarized in Table 1. Among the prepared samples, the B ($x = 0.05$) doped $LiFePO_4/C$ showed the largest bc value. It has been reported that $LiFePO_4/C$ with larger bc value could profit the electrochemical performance due to the enhancement of the diffusion path of lithium ion [2].

The SEM images of the as-prepared ordered $LiFeP_{1-x}B_xO_{4-\delta}/C$ ($x = 0.00$, 0.10) are shown in Fig. 2. As shown in the images, the $LiFePO_4/C$ sample shows a wide particle size distribution of 200–600 nm with the irregular morphology. By contrast, the $LiFeP_{1-x}B_xO_{4-\delta}/C$ ($x = 0.10$) sample shows the smaller particle size in the range of 200–300 nm with the regular ellipsoid morphology. This demonstrates that the doping ions B^{3+} could effectively inhibit

Table 1
Calculated lattice parameters and unit cell volume.

Samples	Lattice constant			Unit cell volume/nm^3
	a/nm	b/nm	c/nm	
$LiFePO_4/C$	0.598497	1.031792	0.468557	0.28935
$LiFeP_{0.95}B_{0.05}O_{4-\delta}/C$	0.600513	1.032989	0.469139	0.29102
$LiFeP_{0.9}B_{0.1}O_{4-\delta}/C$	0.601155	1.033676	0.469535	0.29177
$LiFeP_{0.85}B_{0.15}O_{4-\delta}/C$	0.599835	1.033361	0.469349	0.29117

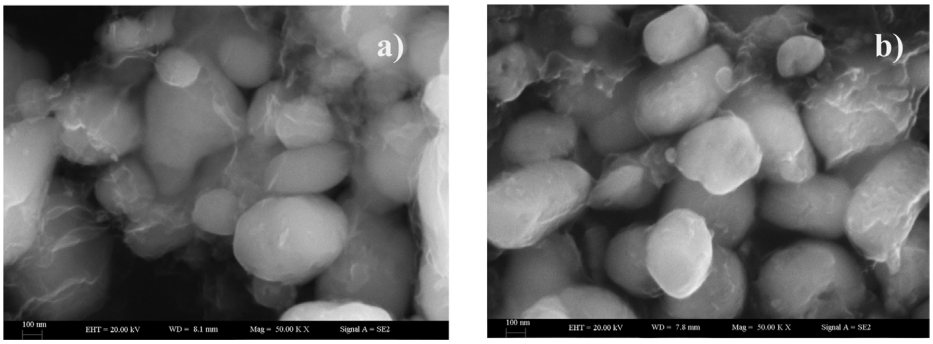

Fig. 2. SEM images of a) the as-prepared $LiFeP_{1-x}B_xO_{4-\delta}/C$ ($x = 0.00$) and b) the as-prepared $LiFeP_{1-x}B_xO_{4-\delta}/C$ ($x = 0.10$).

the growth of $LiFePO_4$ crystal. Reducing the particle size, shorten the diffusion distance of Li ions across the $LiFePO_4/FePO_4$ interface. And, the B^{3+} doping into the crystal can reduce the negative effect on Li^+ ions move in the crystal as the strong bond of the P–O. Consequently, the electrochemical properties of $LiFePO_4$ will be improved effectively via the doping of B ions at the P site as the smooth moving and short diffusion distance of the Li^+ ions. With the increasing of the x value, the particle size of the as-prepared materials has decreased. The morphologies and sizes of the products are related to the status of the carbonate precursor, which will not be discussed in the investigation.

3.2. Electrochemical performance

3.2.1. Rate and cycling stability

The first charge and discharge curves of $LiFeP_{1-x}B_xO_{4-\delta}/C$ ($x = 0.00$, 0.05, 0.10 and 0.15) at 0.2C rate are shown in Fig. 3. All the samples showed the long and flat voltage plateaus at about 3.38–3.38 V, which is the main characteristic of the two-phase reaction of $LiFePO_4$ for lithium extraction and insertion. It is indicating that the well-known crystal $LiFePO_4$ was successfully synthesized and the B doping not destroy the crystal structure of the $LiFePO_4$ in experiment. The polarization potential of these samples are about 0.11 V, 0.09 V, 0.10 V, 0.11 V, respectively, representative of their good kinetics. These data are less than or equal to the value of 0.11 V reported by Xie et al. [17]. And B-doped $LiFePO_4$ in P-site will achieve lower charge and higher discharge plateaus which result in improving the conductivity of composite materials and decreasing the electrode polarization. That's attribution to the short Li^+ ions diffusion distance and high Li^+ ions conductivity as discussed above.

At the same time, with the increase of B^{3+} doping, the first discharge specific capacity firstly increased and then decreased. When $x = 0.1$, the first discharge specific capacity reached maximum value, which exhibits the best electrochemical performance. The first charge specific capacity of $LiFeP_{0.9}B_{0.1}O_{4-\delta}/C$ is 165.1 mAh g^{-1} and the first discharge specific capacity is 155.2 mAh g^{-1}, which is nearly 92% of the theoretical capacity of $LiFePO_4/C$ [17].

High rate performance is one of the significant electrochemical aspects of lithium-ion batteries for high power applications. Fig. 4 shows the charge–discharge curves of the $LiFeP_{0.9}B_{0.1}O_{4-\delta}/C$ at various rates. The sample shows the capacity of 155.2 mAh g^{-1}, 146.2 mAh g^{-1}, 139.4 mAh g^{-1}, 132.4 mAh g^{-1}, 119.1 mAh g^{-1} and 102.6 mAh g^{-1} at the rate of 0.2C, 0.5C, 1.0C, 2.0C, 5.0C, and 10.0C, respectively. It retained about 70% capacity of the 0.2C rate even at the high rate of 10.0C, showed the good high rate performance of the $LiFePO_4$ after the B ions doping at the P site.

The capacity decreases from 155.2 mAh g^{-1} to 102.6 mAh g^{-1} with increasing C-rate from a value of 0.2C to 10C, showing a diffusion-limited mass transfer of Li^+ ions. Upon increasing the C rate, it is seen that the polarization of the electrode material increases, which is reflected in terms of potential of the discharge plateaus. In other words, it shows that the doping of B could improve the electrical properties of $LiFePO_4$, and increase the diffusion coefficient of Li^+ ions.

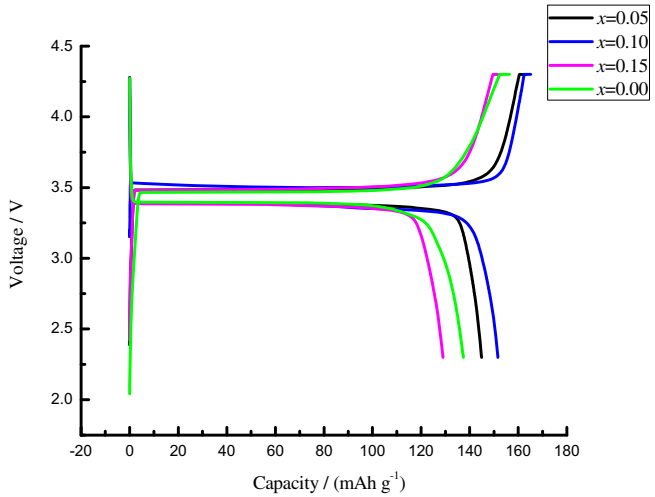

Fig. 3. First charge–discharge curves of $LiFeP_{1-x}B_xO_{4-\delta}/C$ ($x = 0.00$, 0.05, 0.10 and 0.15) at 0.2C.

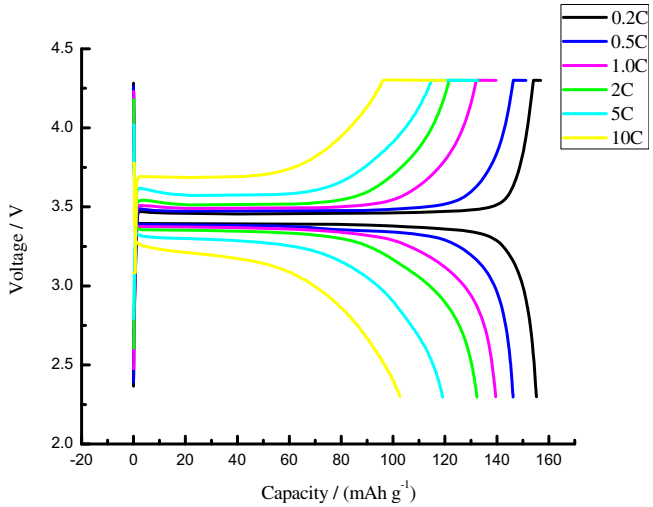

Fig. 4. Charge–discharge curves of $LiFeP_{0.9}B_{0.1}O_{4-\delta}/C$ at various rates.

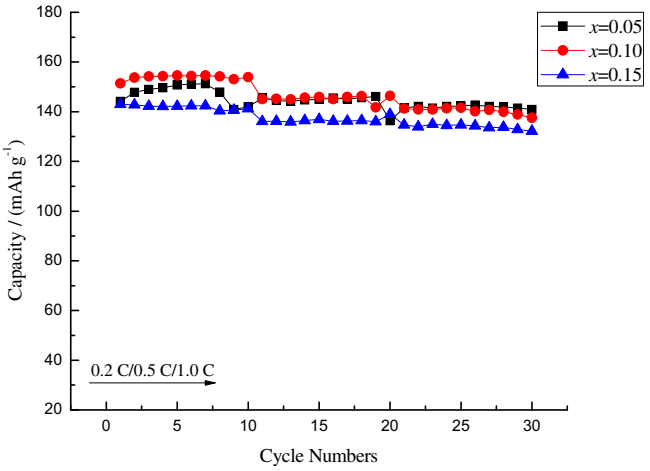

Fig. 5. Cycling performance of $LiFeP_{1-x}B_xO_{4-\delta}/C$ ($x = 0.05$, 0.10 and 0.15).

Fig. 5 shows capacity retention of the cathode $LiFePO_4/C$ at with different B doping contents. In the experiment, the electrode was charged up to 4.3 V at the rate of 0.2C prior to each discharge. Obviously, the sample B ($x = 0.10$) doped $LiFePO_4/C$ exhibits the highest capacity and the best capacity retention during cycling; the discharge capacities are 154.9 mAh g^{-1}, 146.3 mAh g^{-1} and 139.8 mAh g^{-1} at the rate of 0.2C, 5C and 1.0C, with retention ratio of 99.3%, 96.5% and 97.4% after 10 cycles, respectively. With the change of B^{3+} doping, the conductivity of composite materials has been improved, and the cycling performance and rate capability have been enhanced effectively. Although the sample B ($x = 0.05$) doped $LiFePO_4/C$, also delivers a high capacity at 0.5C and 1.0C, the low rate performance is not as good as that of B ($x = 0.10$) doped $LiFePO_4/C$. The ability to exhibit high capacities and retain capacity during cycling is: B ($x = 0.10$) doped $LiFePO_4/C$ > B ($x = 0.05$) doped $LiFePO_4/C$ > B ($x = 0.15$) doped $LiFePO_4/C$ [18].

The differences in the capacity retention between the B-doped $LiFePO_4/C$ materials appeared due to the high chemical affinity of B-doped materials appeared with oxygen, which provided excess current at the 3 V region and stable intercalation at the large current discharge range.

The rate performance of B ($x = 0.00$) doped $LiFePO_4/C$ and B ($x = 0.10$) doped $LiFePO_4/C$ is shown in Fig. 6. Both B ($x = 0.00$) and B

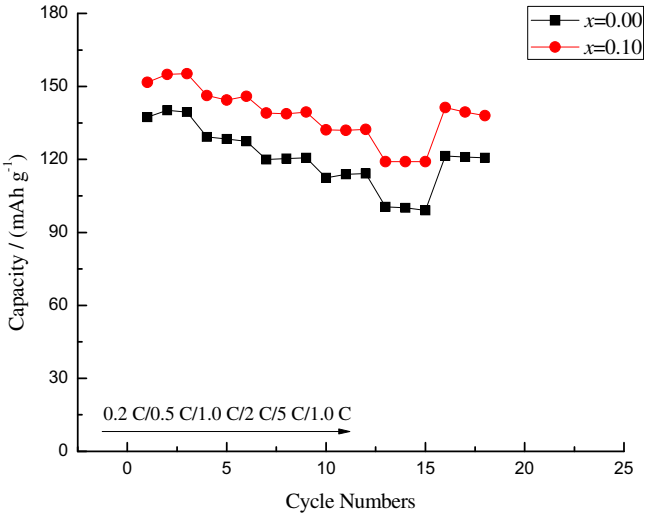

Fig. 6. Rate performance of $LiFeP_{1-x}B_xO_{4-\delta}/C$ ($x = 0.00$, 0.10).

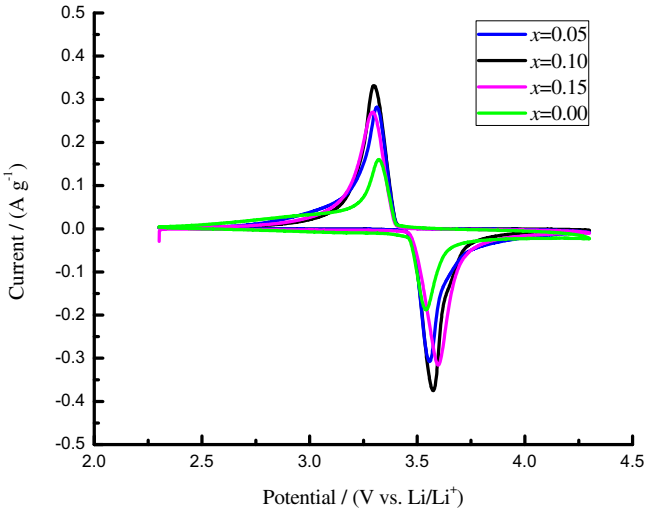

Fig. 7. Cycle voltammograms of the as-prepared $LiFeP_{1-x}B_xO_{4-\delta}/C$ ($x = 0.00$, 0.05, 0.10 and 0.15)/Li cell between 2.3 and 4.3 V vs. Li/Li^+ reference electrode at a scan rate of 0.1 mV s^{-1}.

($x = 0.10$) doped $LiFePO_4/C$ particles exhibit an excellent rate capability. In addition, B ($x = 0.10$) doped $LiFePO_4/C$ displays a better rate capability at various rates, and enhances the cycling performance and rate capability effectively. Furthermore, in cases of B ($x = 0.10$) doped $LiFePO_4/C$ particles, after continuous 3 cycles at different rates of 0.2, 0.5, 1, 2, and 5C, the discharge capacity of 1.0C rate can be reconverted to the previous value. In summary, it supports that the $LiFeP_{0.9}B_{0.1}O_{4-\delta}/C$ have better electrochemical reversibility and structural stability, compared with the other B-doped $LiFePO_4/C$.

3.2.2. CV character

As for CV, the voltage difference between oxidation peak and reduction peak is an important parameter to value the electrochemical reaction reversibility. Fig. 7 shows cyclic voltammograms of the as-prepared $LiFeP_{1-x}B_xO_{4-\delta}/C$ ($x = 0.00$, 0.05, 0.10 and 0.15)/Li cell. As shown in Fig. 7, the oxidation and reduction peak positions for the cell in the initial cycle appear at 3.54 and 3.31 V, 3.57 and 3.30 V, 3.57 and 3.31 V, 3.60 and 3.29 V, vs. Li/Li^+, respectively; the voltage difference between the oxidation and reduction potential is 0.23 V, 0.27 V, 0.26 V, 0.31 V, respectively, the redox peak profiles of $LiFePO_4/Li$ cell are relatively symmetric, which demonstrate that the electrochemical reaction reversibility of LFP/Li cell is fairly excellent. The distance between the oxidation peak and reduction peak is quite small, indicating that the electrochemical polarization of the materials is very weak. Among them, the $LiFeP_{0.9}B_{0.1}O_{4-\delta}/C$ displays smaller distance between the oxidation peak and reduction peak, and larger areas surrounded by CVs, implying that the $LiFeP_{0.9}B_{0.1}O_{4-\delta}/C$ has better electrochemical reversibility, battery reaction kinetic and rate performance.

4. Conclusions

In conclusion, the B-doped $LiFePO_4$ in P-site, $LiFeP_{1-x}B_xO_{4-\delta}/C$ ($x = 0.00$, 0.05, 0.10 and 0.15) composite materials were successfully synthesized in flowing N_2 atmosphere by liquid phase reduction method with heat treatment.

1) Analysis from XRD shows that as-prepared materials have well-regulated olivine-type structures, high crystallinity.

2) Further investigation conducted with SEM confirmed that the prepared composite material had sub-micrometric particle size and homogeneous particle size distribution.
3) It is found that B doped at P sites is feasible and significant. With the increase of B^{3+} doping, the first discharge specific capacity firstly increased and then decreased. When $x = 0.1$, the first discharge specific capacity reached maximum value, which exhibits the best electrochemical performance. The discharge capacities of $LiFeP_{0.9}B_{0.1}O_{4-\delta}/C$ synthesized are 155.2 mAh g^{-1}, 146.2 mAh g^{-1}, 139.4 mAh g^{-1}, 132.4 mAh g^{-1}, 119.1 mAh g^{-1} and 102.6 mAh g^{-1} at the rate of 0.2C, 0.5C, 1.0C, 2.0C, 5.0C, and 10.0C. After continuous 3 cycles at different rates of 0.2, 0.5, 1.0, 2.0, 5.0 and 10.0C, the discharge capacity of 1.0C can reconvert to the previous value.

Acknowledgments

We are grateful to the financial support of the Science and Technology Projects of Urumqi (No. K111410005), the West Light Foundation of the Chinese Academy of Sciences (No. XB200919), and the Knowledge Innovation Program of the Chinese Academy of Sciences (No. 20092A401).

References

[1] K.S. Nanjundaswamy, A.K. Padhi, J.B. Goodenough, S. Okada, H. Ohtsuka, H. Arai, J. Yamaki, Solid State Ionics 92 (1996) 1–10.
[2] J.M. Tarascon, M. Armand, Nature 414 (2001) 359–367.
[3] A.K. Padhi, K.S. Nanjundaswamy, J.B. Goodenough, Journal of the Electrochemical Society 144 (1997) 1188–1194.
[4] D.K. Kim, H.M. Park, S.J. Jung, Journal of Power Sources 159 (2006) 237–240.
[5] M. Isono, S. Okada, J. Yamaki, Journal of Power Sources 195 (2010) 593–598.
[6] Z.Y. Tang, F. Gao, J.J. Xue, Journal of Inorganic Materials 23 (2008) 1188–1194.
[7] S.Y. Chung, Y.M. Chiang, Electrochemical and Solid-State Letters 6 (2003) 278–281.
[8] M.R. Yang, W.H. Ke, Journal of the Electrochemical Society 155 (2003) 729–732.
[9] J. Barker, M.Y. Saidi, J.L. Swoyer, Electrochemical and Solid-State Letters 6 (2003) 53–55.
[10] F.L. Liu, S.C. Han, H. Chan, Chinese Journal of Power Sources 33 (2009) 339–400.
[11] Y.X. Wen, J.P. Zheng, Z.F. Tong, Inorganic Chemicals Industry 4 (2005) 12–14.
[12] Y.R. Zhang, W.J. Wang, Journal of Inorganic Materials 19 (2004) 349–353.
[13] A. Yamada, N. Iwane, Y. Harada, Journal of Advanced Materials 22 (2010) 3583–3587.
[14] V. Legagneur, Solid State Ionics 139 (2001) 37–46.
[15] Z.G. Ren, M.Z. Qu, Z.L. Yu, Journal of Inorganic Materials 25 (2010) 230–234.
[16] Y.Z. Dong, Y.M. Zhao, Z.D. Shi, Electrochimica Acta 53 (2008) 2339–2345.
[17] H. Xie, Z.T. Zhou, Journal of Inorganic Materials 22 (2007) 631–636.
[18] X. Fang, Y. Lu, N. Ding, Electrochimica Acta 55 (2010) 832–837.